

SUPPORTING INFORMATION

Modular Architecture and Unique Teichoic Acid Recognition Features of Choline-Binding Protein L (CbpL) Contributing to Pneumococcal Pathogenesis

Javier Gutiérrez-Fernández,^{1,5,6} Malek Saleh,^{2,5,6} Martín Alcorlo,^{1,5} Alejandro Gómez M.,² David Pantoja-Uceda,³ Miguel A. Treviño,³ Franziska Voß,² Mohammed R. Abdullah,² Sergio Galán-Bartual,^{1,6} Jolien Seinen,² Pedro A. Sánchez-Murcia,⁴ Federico Gago,⁴ Marta Bruix,³ Sven Hammerschmidt^{2*} and Juan A. Hermoso^{1*}

(1) Department of Crystallography and Structural Biology, “Rocasolano” Institute of Physical-Chemistry, CSIC, Serrano 119, E-28006-Madrid, Spain.

(2) Department Genetics of Microorganisms, Interfaculty Institute for Genetics and Functional Genomics, Ernst Moritz Arndt University of Greifswald, D-17487 Greifswald, Germany.

(3) Department of Biological Physical Chemistry. “Rocasolano” Institute of Physical-Chemistry, CSIC, Serrano 119, E-28006-Madrid, Spain.

(4) Department of Biomedical Sciences, Unidad Asociada al IQM-CSIC, Universidad de Alcalá, E-28871 Alcalá de Henares, Madrid, Spain.

(5) These authors contributed equally to this work.

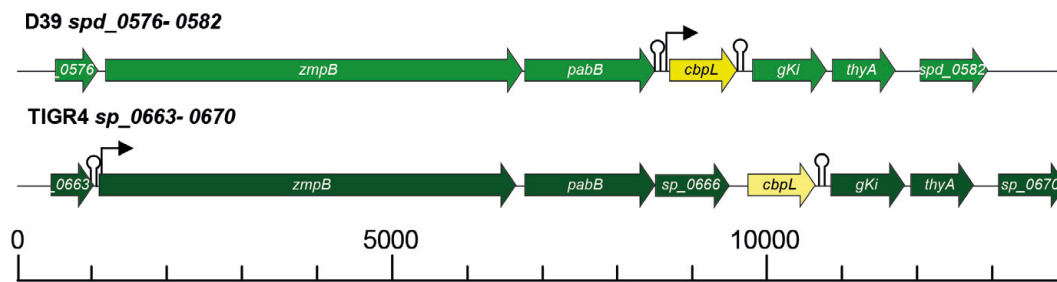
(6) Present address: J G-F: Institute of Science and Technology Austria (IST Austria), Am Campus 1, 3400 Klosterneuburg, Austria; MS: Institut für Biologie – Mikrobiologie, Freie Universität Berlin, 14195 Berlin, Germany; S G-B: School of Life Sciences, University of Dundee, Dundee, UK.

10	20	30	40	50	60
MNKRLFSKMS	LVTLPILALF	SQSVLAEENI	HFSSCKEAWA	NGYSDIHEGE	PGYSAKLDRD
70	80	90	100	110	120
HDGVACELKN	APKGAFKAKQ	STAIQINTSS	<u>ATTSGWVKQD</u>	<u>GAWYYFDGNG</u>	<u>NLVKNAWQGS</u>
				R1	
130	140	150	160	170	180
<u>YYLKADGKMA</u>	<u>QSEWIYDSSY</u>	<u>QAWYYLKSDG</u>	<u>SYAKNAWQGA</u>	<u>YYLKSNKMA</u>	<u>QGEWYDSSY</u>
R2		R3		R4	
190	200	210	220	230	240
<u>QAWYYLKSDG</u>	<u>SYARNAWQGN</u>	<u>YYLKSDGKMA</u>	<u>KGEWYDATY</u>	<u>QAWYYLTSYG</u>	<u>SYAYSTWQGN</u>
R5		R6		R7	
250	260	270	280	290	300
<u>YYLKSDGKMA</u>	<u>VNEWVDGGRY</u>	<u>YVGADGVWKE</u>	<u>VQASTASSSN</u>	<u>DSNSEYSAAL</u>	<u>GKAKSYNSLF</u>
R8		R9			
310	320	330			
<u>HMSKKRMYRQ</u>	<u>LTSDFDKFSN</u>	<u>DAAQY AIDHL</u>	<u>DD</u>		

Fig. S1. Amino acid sequence of CbpL.

Color code for the different parts of the protein is as follows: signal peptide (gray), Excalibur domain (green), linkers (black), choline binding domain (CBD, purple), Ltp_Lipoprotein domain (red). Sequence of the choline binding repeats (R1 to R9) integrating the CBD is underlined in different colors.

A Gene organization of *cbpL* in *S. pneumoniae*



B *S. pneumoniae* D39 *cbpL*-mutants

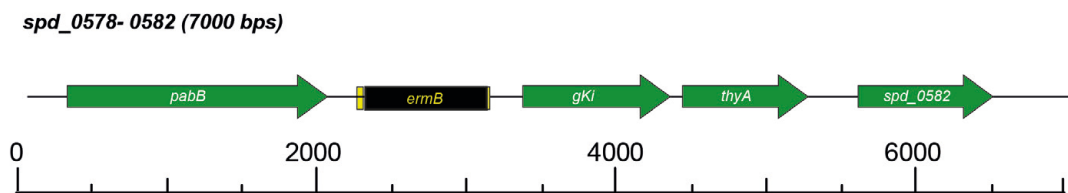


Fig. S2. Molecular organization of the *cbpL*-gene loci in *Streptococcus pneumoniae* D39 and TIGR4.

(A) The *in silico* analysis revealed a monocistronic organization of the CbpL-encoding gene in D39 and a polycistronic organization in TIGR4. The protein accession is YP_816078.1. The two genes upstream of *cbpL* in D39 encode a zinc metalloprotease (ZmpB; SPD_0577 in D39) and a *para*-aminobenzoic acid synthetase (PabB; SPD_0578 in D39). The genes downstream of *cbpL* encode a glucokinase (Gki; SPD_0580) and thymidylate synthase (ThyA; SPD_0581), respectively. In TIGR4 the gene *sp_0666* is annotated between *cbpL* and *pabB* and suggested to encode a putative pyrimidine utilization protein [1]. Putative promoters (arrows) were predicted by the Neural Network Promoter Prediction program (http://www.fruitfly.org/seq_tools/promoter.html) and potential rho-independent termination sequences were extracted from the TransTermHP Terminator Prediction list of *S. pneumoniae* D39 (http://transterm.cbcb.umd.edu/tt/Streptococcus_pneumoniae_D39.tt). The sequences

were obtained from the Kyoto Encyclopedia for Genes and Genomes (KEGG). **(B)** Mutants deficient in CbpL-expression were constructed by deletion-insertion mutagenesis. This resulted in a complete deletion of the *cbpL* gene sequence and insertion of an *ermB* gene cassette.

Pneumococcal CbpL protein sequence alignment

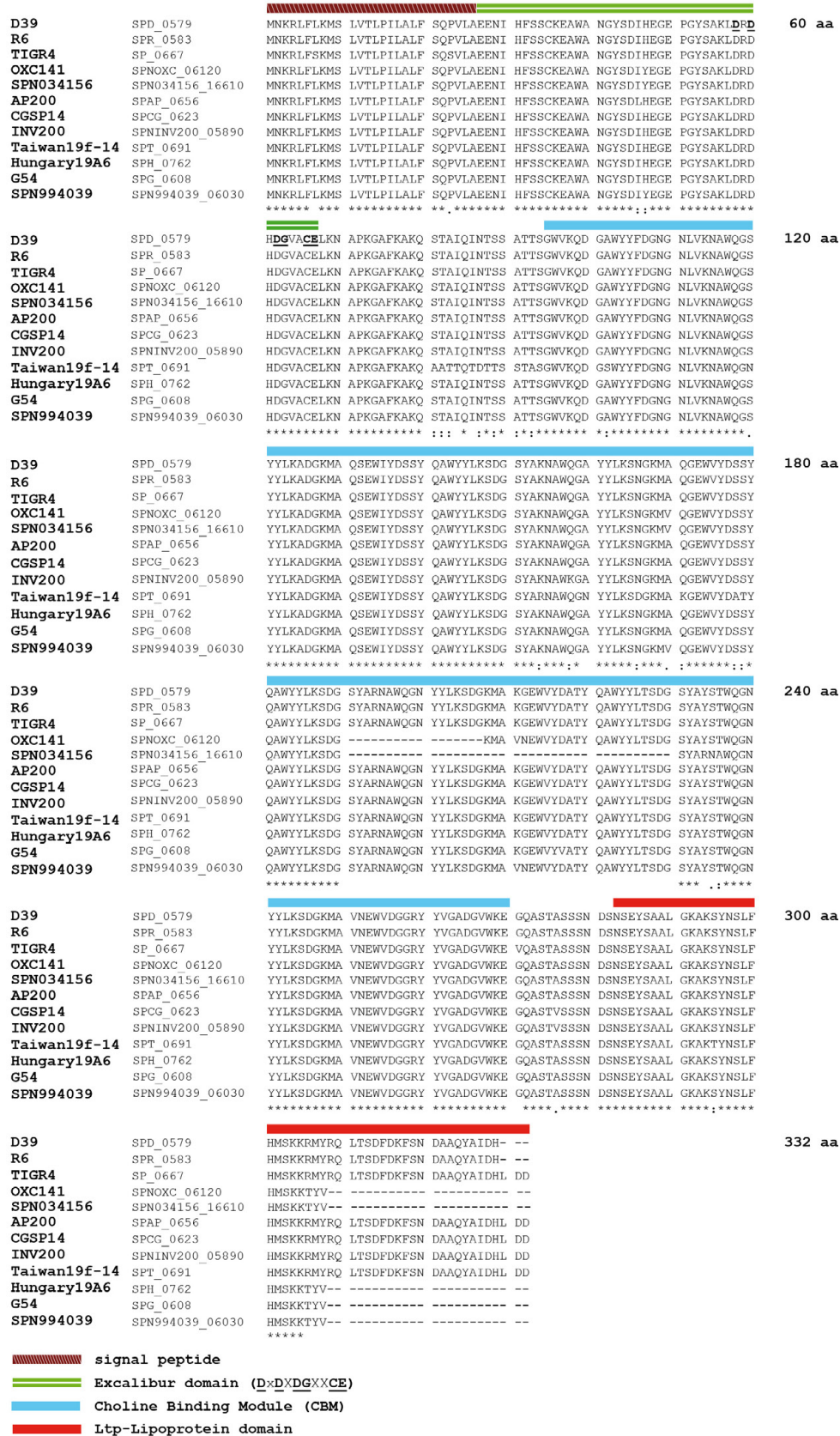
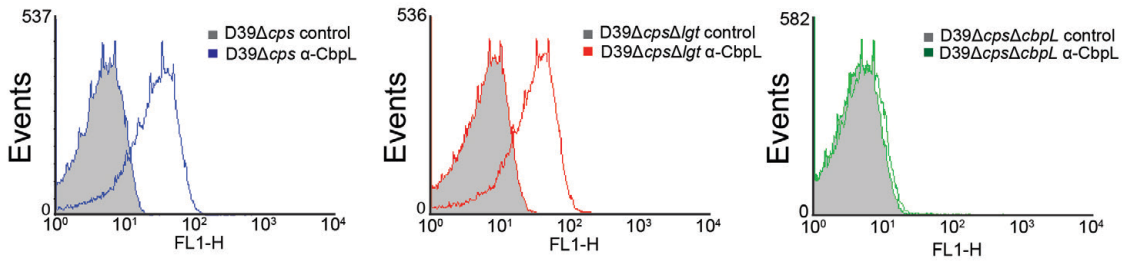
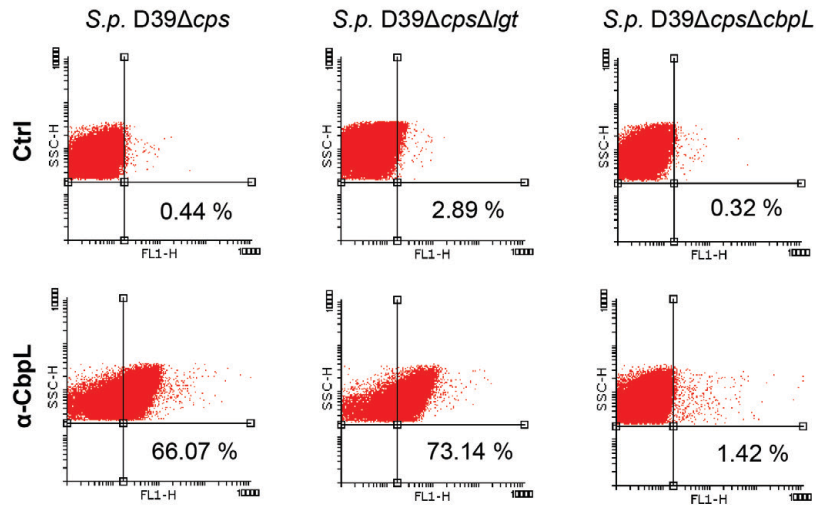
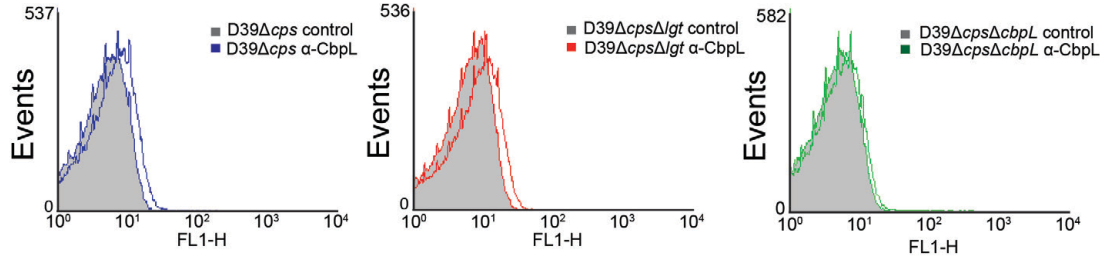
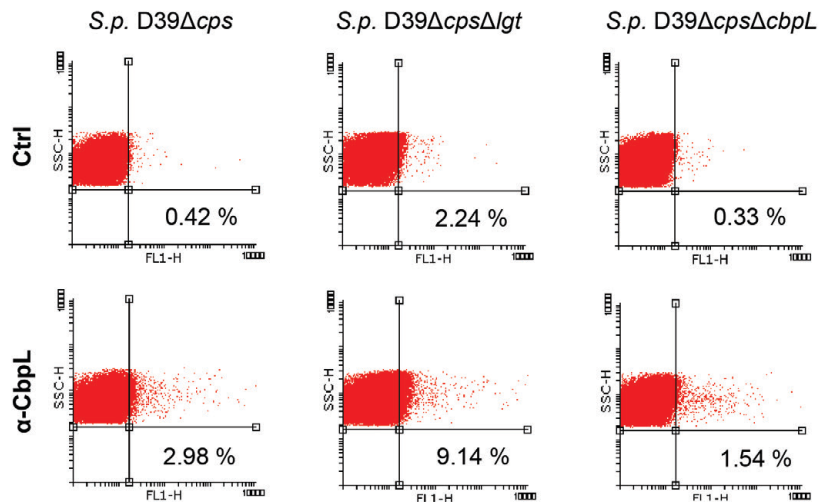


Fig. S3. Multiple amino acid sequence alignment of pneumococcal CbpL.

Alignment performed with Clustal Omega alignment tool (<http://www.ebi.ac.uk/Tools/msa/clustalo/>) with *cbpL* sequences as deposited in databases for 12 strains.

A**B****C****D**

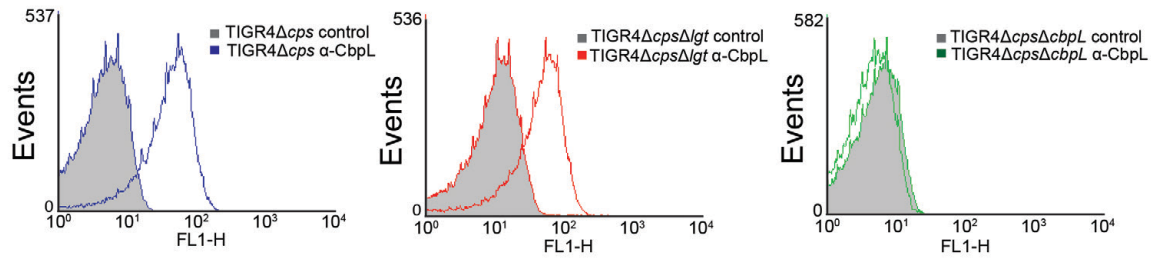
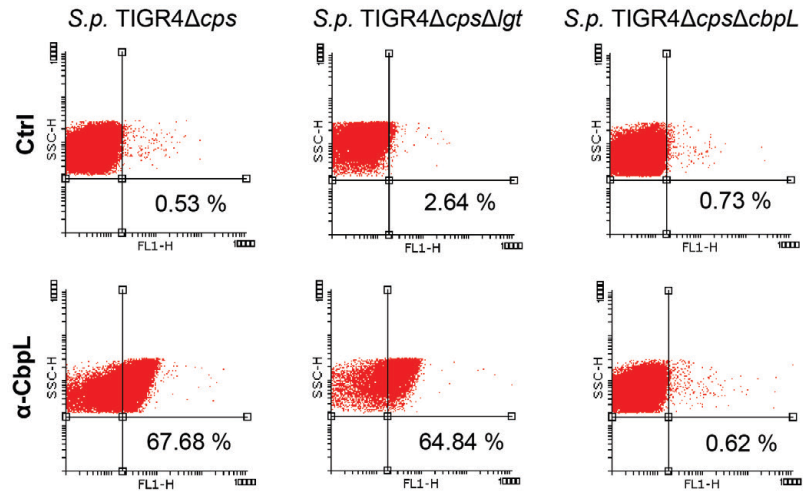
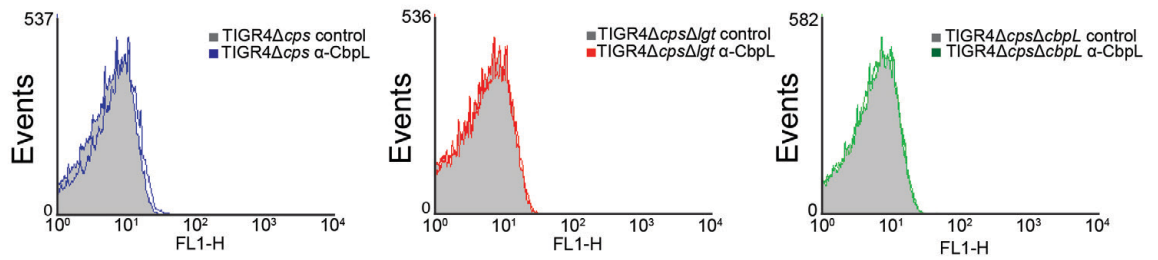
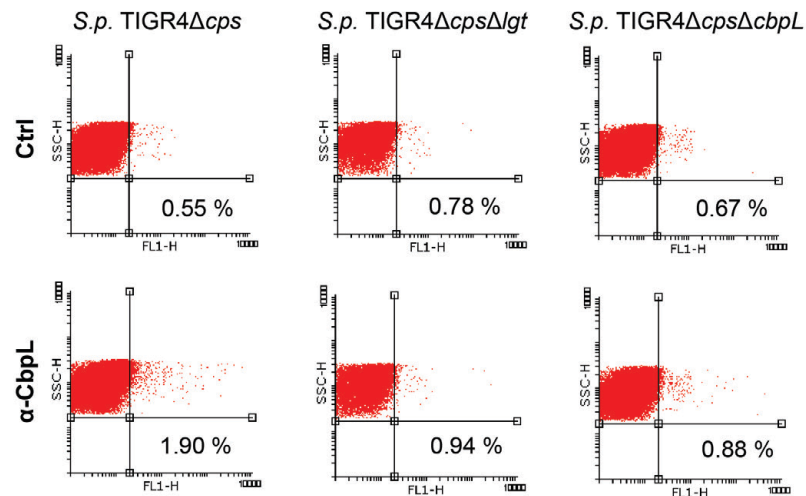
E**F****G****H**

Fig. S4. Surface abundance of CbpL determined by flow cytometry.

The surface abundance of CbpL was measured by flow cytometry using anti-CbpL polyclonal antibodies (1:500) as primary antibodies and secondary goat anti-mouse IgG coupled Alexa-Fluor-488 (1:1000; Invitrogen). The non-encapsulated D39 Δ *cps* (**A – D**) or TIGR4 Δ *cps* (**E – H**) and their isogenic *lgt*- and *cbpL* mutants were incubated with the antibodies and the fluorescence intensity measured in a FACSCalibur™. The surface abundance of CbpL was measured prior (**A – B** and **E – F**) and post-treatment (**C – D** and **G – H**) of pneumococci with choline chloride (10% ChCl for 30 min). The individual histograms showing the increase in fluorescence intensity (forward scatter: FL1-H) for each strain tested (control: only the secondary anti-mouse IgG Alexa-Fluor conjugate antibody; CbpL detection: incubation with 1st and 2nd antibodies) are shown in **A, C, E, and G**. Dot plots of the flow cytometric analyses including the percent of positive events when counting 50000 events are shown in **B, D, F, and H**.

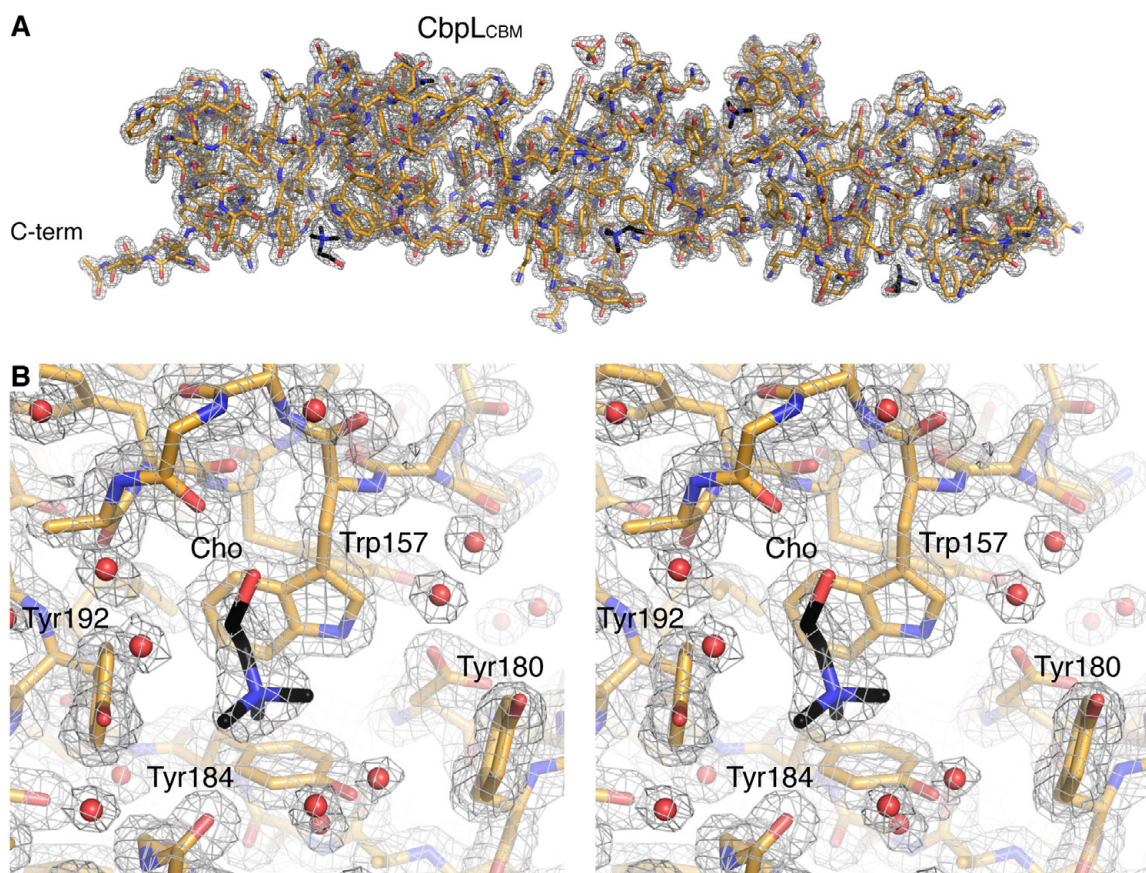


Fig. S5. Electron density in CbpL_{CBM}.

(A) Electron density map for the complete CbpL_{CBM}:choline complex. (B) Stereo view showing a detail of the electron density map in a non-canonical choline-binding site. Residues interacting with choline are represented as capped sticks and labeled. Water molecules represented as red spheres. Electron density maps correspond to the σ -weighted $2F_o - F_c$ electron density map contoured at 1.0σ .

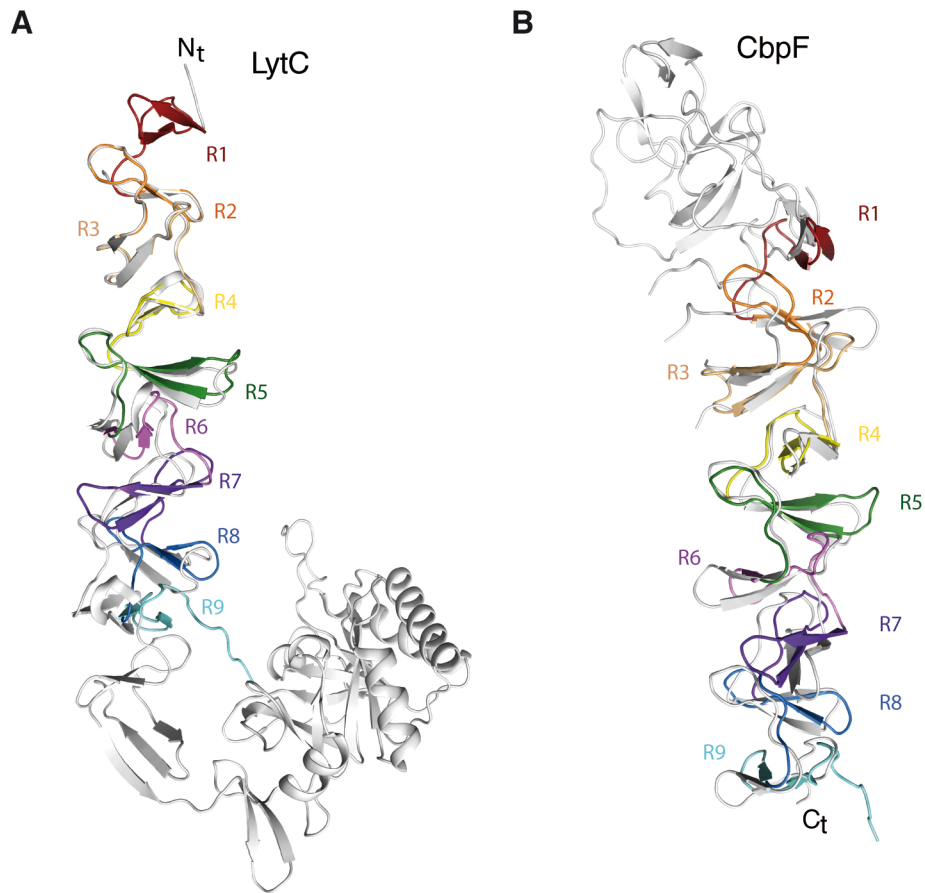


Fig. S6. Structural comparison of CbpL_{CBM} with closest structural homologues.

(A) Structural superimposition of pneumococcal autolysin LytC (colored in grey) (PDB code 2WWD) with CbpL_{CBM} (each repeat colored differently) results in a rmsd of 1.9 Å for 155 C α atoms. (B) Structural superimposition of pneumococcal CbpF (colored in grey) (PDB code 2V05) with CbpL_{CBM} (each repeat colored differently) results in a rmsd of 3.1 Å for 173 C α atoms.

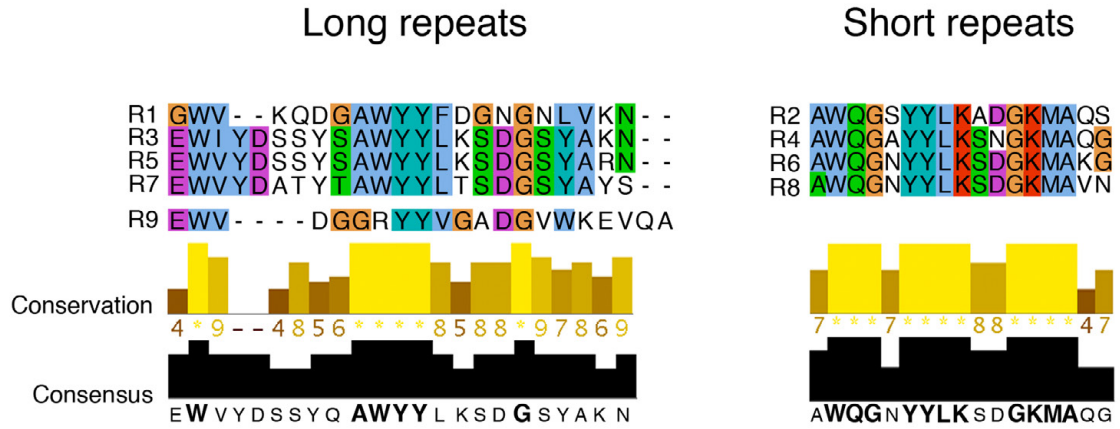


Fig. S7. Sequence comparison of choline-binding repeats in CbpL.

Long choline-binding repeats (left) and short choline-binding repeats (right) in CbpL are compared. Sequence alignments were performed with Clustal Omega and visualized using Jalview. R9 was not considered for the alignments.

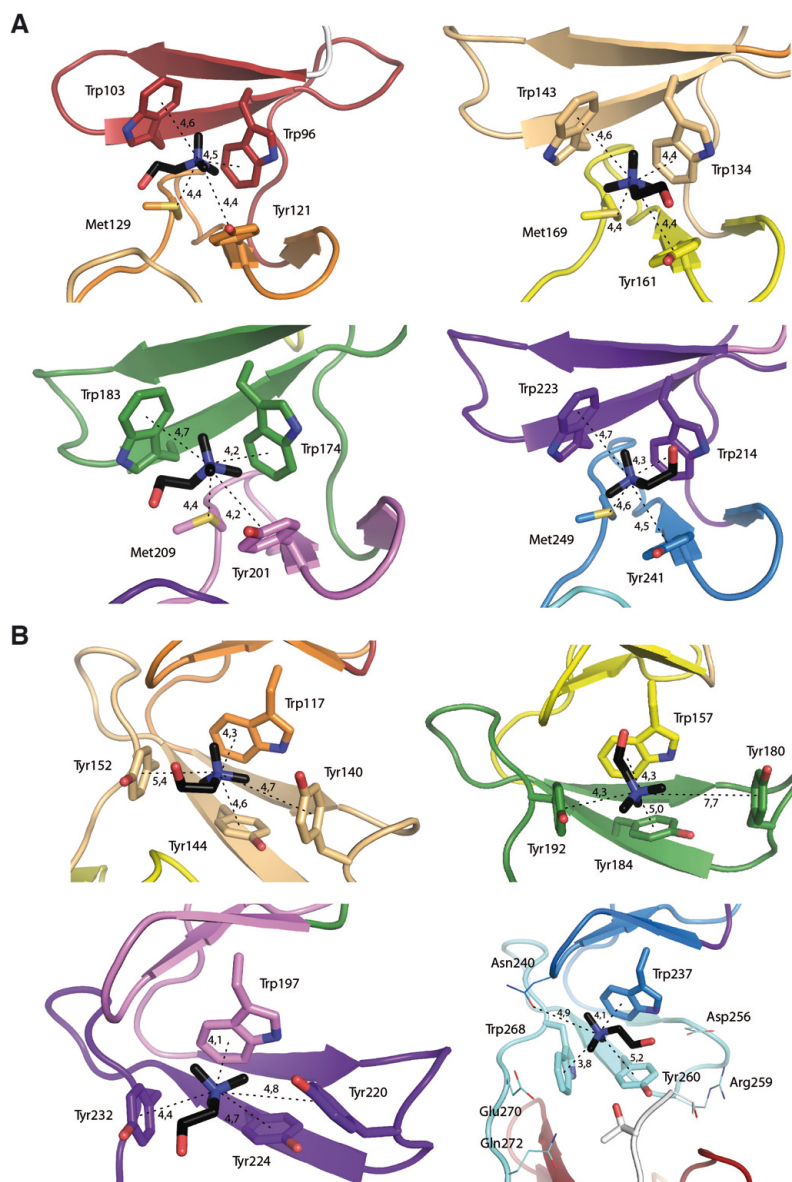


Fig. S8. Structural description of choline-binding sites in CbpL.

(A) The four canonical choline-binding sites present in CbpL (repeats are colored as in Fig 3). (B) The four non-canonical choline-binding sites present in CbpL (colored as in Fig 3) with main residues involved in choline stabilization depicted as capped sticks. Choline moieties attached to the choline-binding sites are represented as capped sticks with C atoms in black.

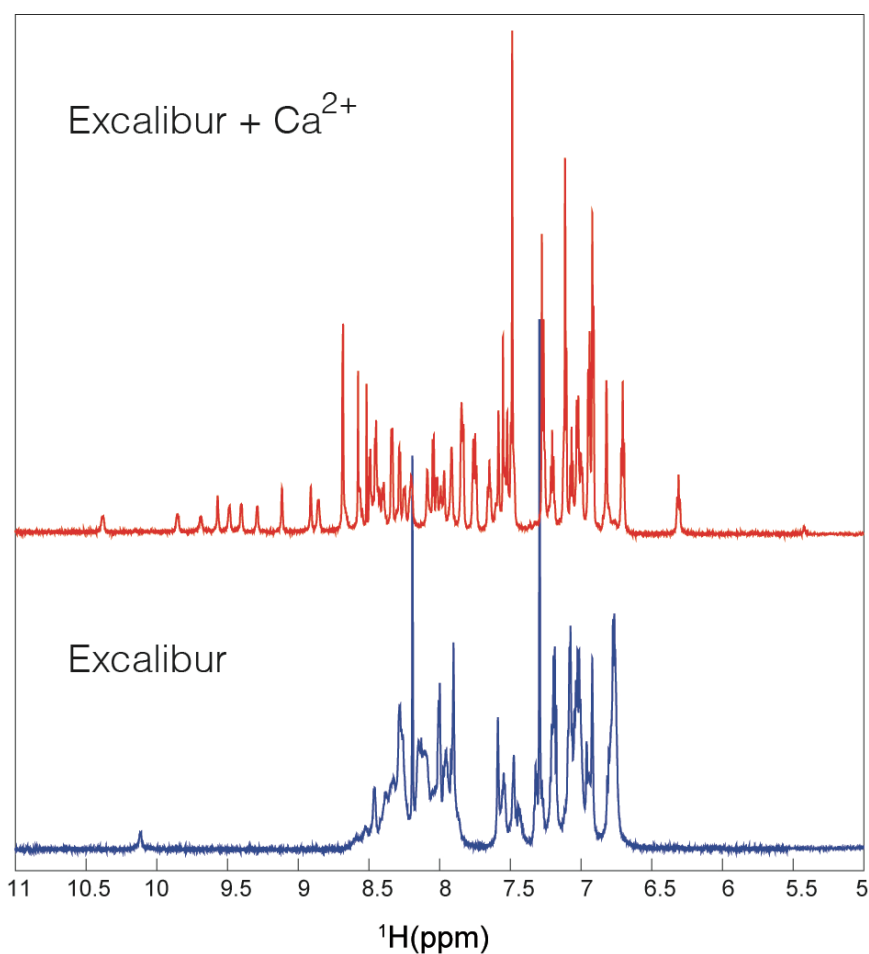


Fig. S9. Folding of the Excalibur domain requires Ca^{2+} binding.

NH region of the ^1H NMR spectra of Excalibur, 0.5 mM, pH 5.5, 800 MHz. Without Ca^{2+} the spectrum (colored in blue) shows severe signal overlapping in a narrow chemical shift range compatible with an unfolded peptide conformation. The same spectrum saturated with Ca^{2+} (colored in red) shows a large signal dispersion characteristic of a folded structure.

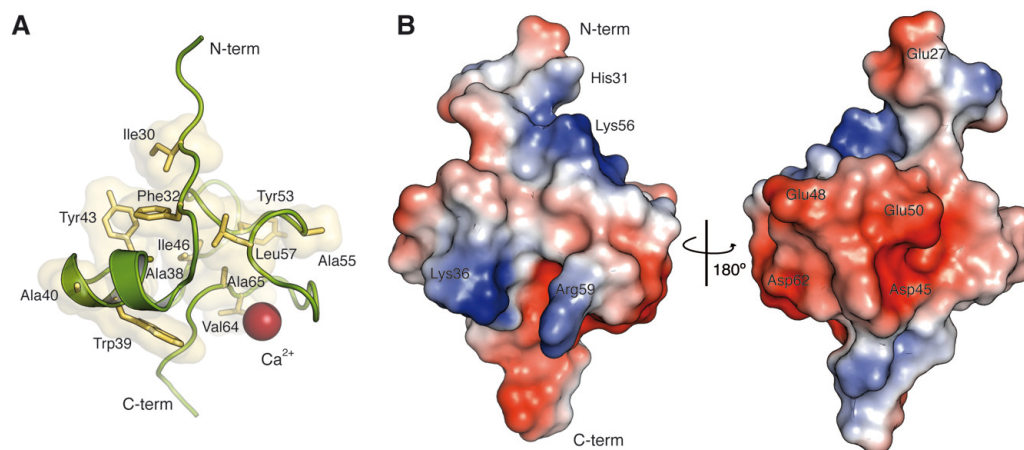


Fig. S10. Structural features of the Excalibur domain.

(A) A strong hydrophobic core is built with aromatic and hydrophobic residues, some of them are exposed. (B) Electrostatic potential surface of the Excalibur domain presents two faces, one of them with prevalence of positively-charged residues and the other (roughly 180° apart) presenting negatively-charged residues.

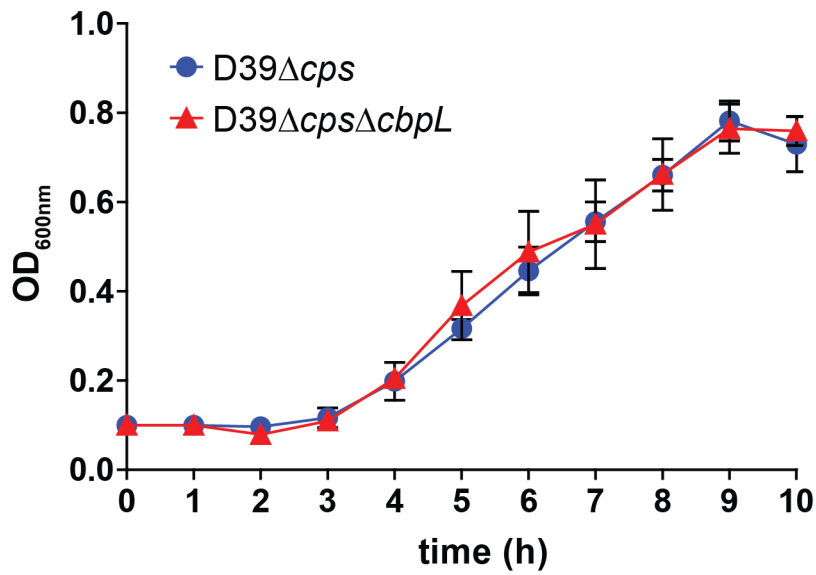


Fig. S11. Growth of pneumococci is not affected in pneumococci lacking CbpL. Pneumococci were cultured in the chemically defined medium RPMI_{modi} [2] under microaerophilic conditions at 37 °C. At each indicated time point the optical density of the culture was measured at 600 nm.

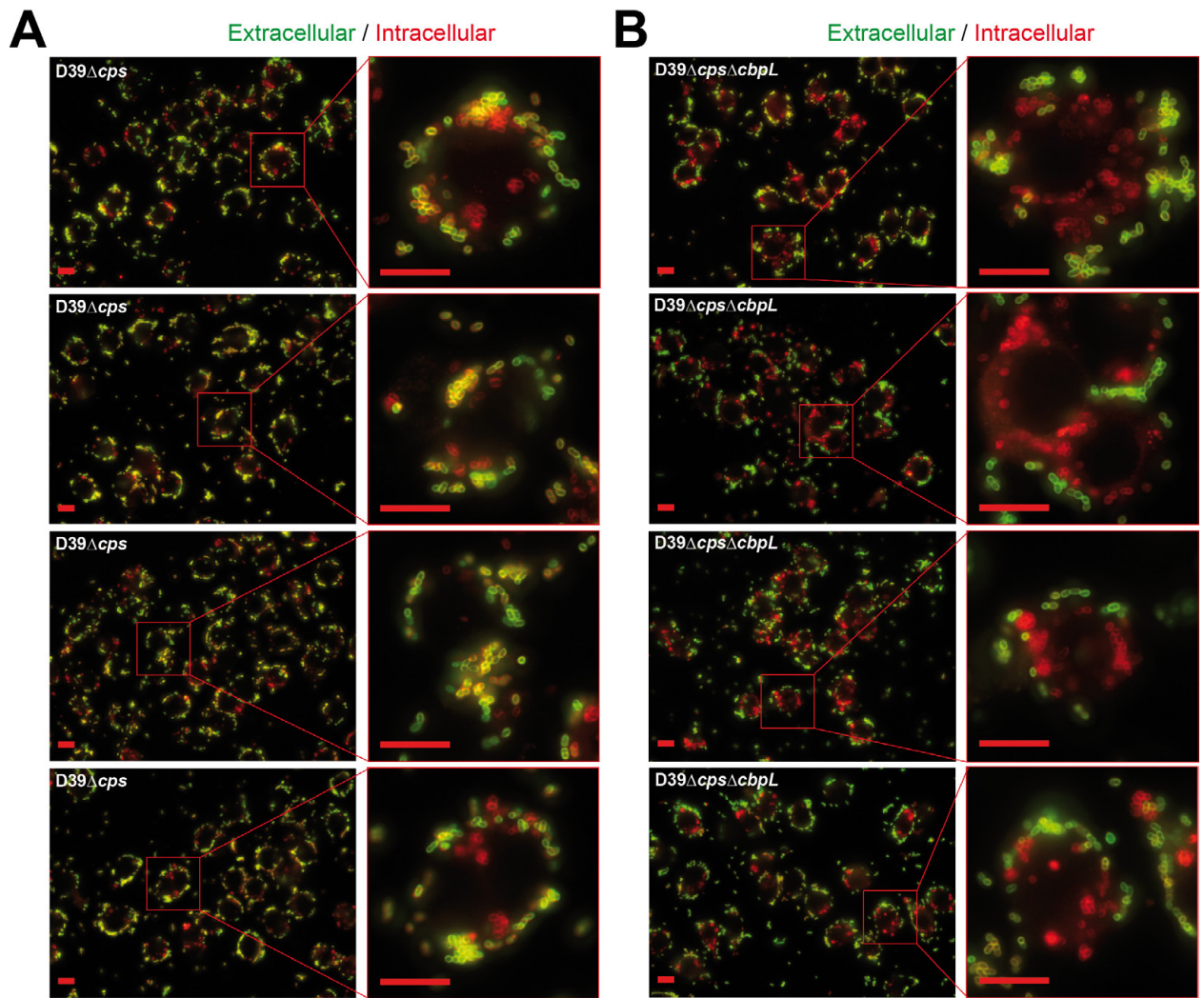


Fig. S12. Immunofluorescence microscopy of macrophage-associated and phagocytosed pneumococci.

Representative immunofluorescence microscopic images of D39 Δ *cps* (**A**) and CbpL-deficient D39 Δ *cps* Δ *cbpL* (**B**) pneumococci attached (green) to J774 macrophages and internalized by J774 macrophages (red) 30 min post infection with an MOI of 50 bacteria per macrophage. Extracellular pneumococci were stained with goat anti-rabbit Alexa Fluor 488 (green) after using anti-pneumococcal polyclonal antibodies as the first antibody, while intracellular pneumococci were stained after Triton™ X-100 permeabilization with goat anti-rabbit Alexa Fluor 568 (red) post Triton X-100

treatment using again rabbit anti-pneumococcal polyclonal antibodies as the first antibody. Bar represents 10 μ m.

CbpL_ltp	EYSAALGKAKSYNSLPHMSKKRMYRQLTSDFDKFSNDAAQYAIIDLDD
4eqq_ltp	EYRTAVSKAKQYASTVHMSKEELRSQVLS-FDKYSQDASDYAVENSGD

50% identity
66.7% similarity

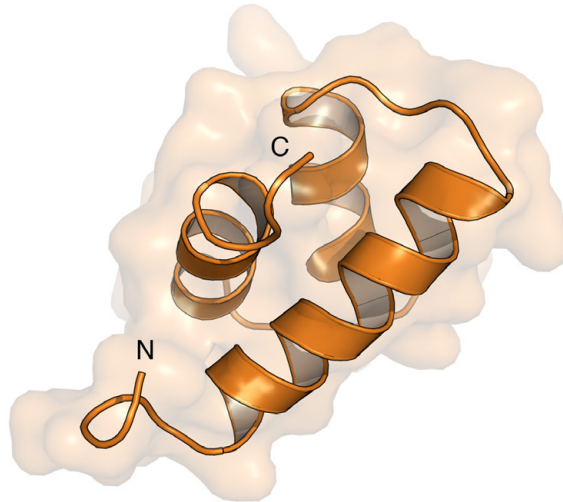


Fig. S13. Homology modeling of CbpL Ltp_Lipoprotein domain.

Homology modeling was performed using the online Swiss-Prot server using Ltp_{TP-J34} protein (PDB code 4EQQ) from temperate phage TP-J34 of *Streptococcus thermophilus* as template [3-5]. Sequence alignment was performed using ClustalW.

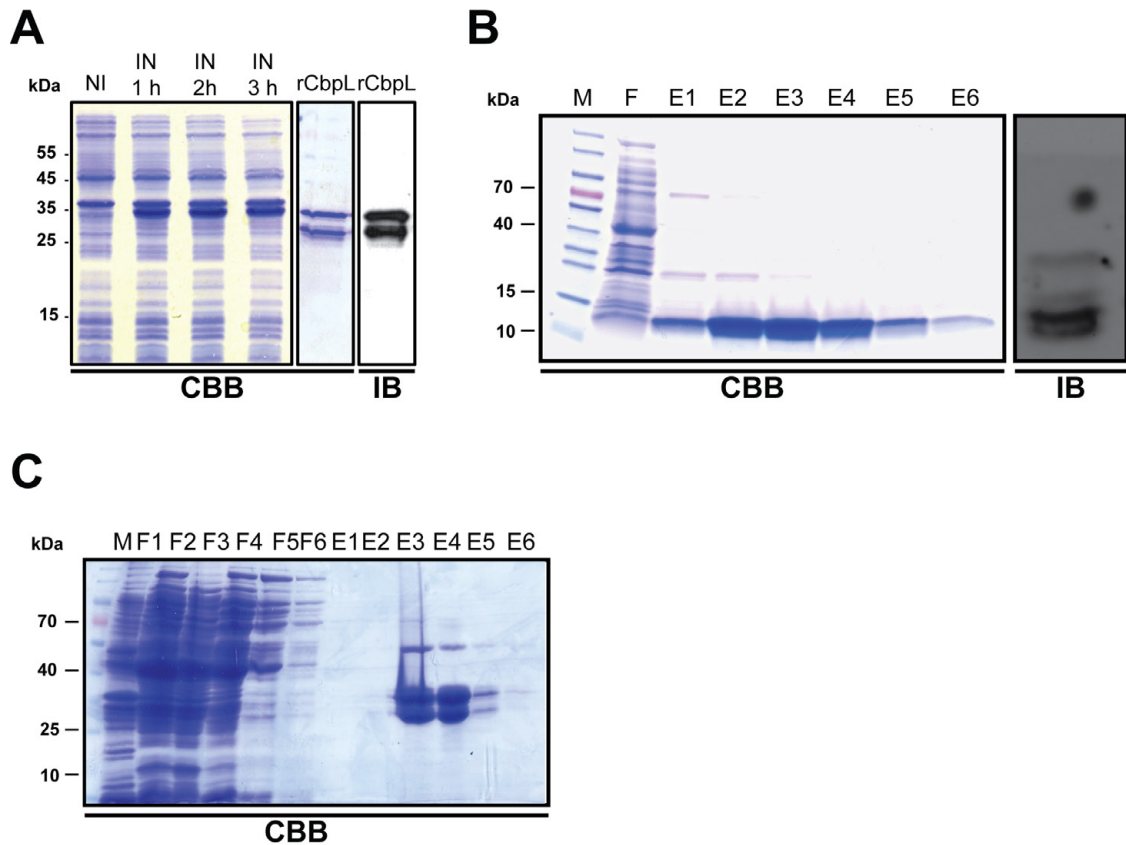


Fig. S14. Heterologous expression and purification of His₆-tagged CbpL, His₆-tagged Excalibur domain, and His₆-tagged Excalibur-CBM domain of CbpL.

(A) Heterologous expression of CbpL lacking the signal peptide (aa 27-332), (B) Excalibur domain (aa 27-70), and (C) Excalibur-CBM (aa 27- 270) cloned into expression vector pTP1 and induced with 1 mM IPTG. The His₆-tag of the purified proteins was removed by cleavage with the TEV protease. The proteins were stained with Comassie brilliant blue (CBB) and the immunoblots (IB) were performed with anti-CbpL polyclonal antibodies generated against rCbpL. NI, non-induced; IN, induced; rCbpL, recombinant without His₆-tag. F: flow through and E: protein elution fractions.

References

- 1 Chimalapati, S. *et al.* Infection with Conditionally Virulent *Streptococcus pneumoniae* Delta pab Strains Induces Antibody to Conserved Protein Antigens but Does Not Protect against Systemic Infection with Heterologous Strains. *Infect Immun* **79**, 4965-4976, doi:10.1128/iai.05923-11 (2011).
- 2 Schulz, C. *et al.* Regulation of the arginine deiminase system by ArgR2 interferes with arginine metabolism and fitness of *Streptococcus pneumoniae*. *MBio* **5**, doi:10.1128/mBio.01858-14 (2014).
- 3 Arnold, K., Bordoli, L., Kopp, J. & Schwede, T. The SWISS-MODEL workspace: a web-based environment for protein structure homology modelling. *Bioinformatics* **22**, 195-201, doi:10.1093/bioinformatics/bti770 (2006).
- 4 Guex, N. & Peitsch, M. C. SWISS-MODEL and the Swiss-PdbViewer: an environment for comparative protein modeling. *Electrophoresis* **18**, 2714-2723, doi:10.1002/elps.1150181505 (1997).
- 5 Guex, N., Peitsch, M. C. & Schwede, T. Automated comparative protein structure modeling with SWISS-MODEL and Swiss-PdbViewer: a historical perspective. *Electrophoresis* **30 Suppl 1**, S162-173, doi:10.1002/elps.200900140 (2009).
- 6 Saleh, M. *et al.* Molecular architecture of *Streptococcus pneumoniae* surface thioredoxin-fold lipoproteins crucial for extracellular oxidative stress resistance and maintenance of virulence. *EMBO Mol Med* **5**, 1852-1870, doi:10.1002/emmm.201202435 (2013).
- 7 Holmes, A. R. *et al.* The pavA gene of *Streptococcus pneumoniae* encodes a fibronectin-binding protein that is essential for virulence. *Mol Microbiol* **41**, 1395-1408 (2001).
- 8 Tettelin, H. *et al.* Complete genome sequence of a virulent isolate of *Streptococcus pneumoniae*. *Science* **293**, 498-506, doi:10.1126/science.1061217 (2001).
- 9 Oggioni, M. R. *et al.* Pneumococcal zinc metalloproteinase ZmpC cleaves human matrix metalloproteinase 9 and is a virulence factor in experimental pneumonia. *Mol Microbiol* **49**, 795-805 (2003).
- 10 Tomasz, A. & Hotchkiss, R. D. Regulation of the Transformability of Pneumococcal Cultures by Macromolecular Cell Products. *Proc Natl Acad Sci USA* **51**, 480-487 (1964).
- 11 Bagnoli, F. *et al.* A second pilus type in *Streptococcus pneumoniae* is prevalent in emerging serotypes and mediates adhesion to host cells. *J Bacteriol* **190**, 5480-5492, doi:10.1128/JB.00384-08 (2008).
- 12 Rennemeier, C. *et al.* Thrombospondin-1 promotes cellular adherence of gram-positive pathogens via recognition of peptidoglycan. *FASEB J* **21**, 3118-3132, doi:10.1096/fj.06-7992com (2007).
- 13 Jensch, I. *et al.* PavB is a surface-exposed adhesin of *Streptococcus pneumoniae* contributing to nasopharyngeal colonization and airways infections. *Mol Microbiol* **77**, 22-43, doi:10.1111/j.1365-2958.2010.07189.x (2010).
- 14 Pribyl, T. *et al.* Influence of impaired lipoprotein biogenesis on surface and exoproteome of *Streptococcus pneumoniae*. *J Proteome Res* **13**, 650-667, doi:10.1021/pr400768v (2014).
- 15 Schulz, C. *et al.* Regulation of the arginine deiminase system by ArgR2 interferes with arginine metabolism and fitness of *Streptococcus pneumoniae*. *MBio* **5**, doi:10.1128/mBio.01858-14 (2014).

- 16 Hammerschmidt, S., Tillig, M. P., Wolff, S., Vaerman, J. P. & Chhatwal, G. S. Species-specific binding of human secretory component to SpsA protein of *Streptococcus pneumoniae* via a hexapeptide motif. *Mol Microbiol* **36**, 726-736 (2000).

Table S1. Strain and plasmid list

Strain or plasmid	Serotype and relevant Genotype ^a	Resistance	Source or Reference
<i>Streptococcus pneumoniae</i>			
SP37	35A	None	NCTC10319
SP39	3	None	ATCC 6303
SP70	12F	None	MUD ^b [6]
SP129	19F	None	MUD ^b [6]
SP173 (R800)	NC ^c	None	[7]
SP257 (D39)	2	None	NCTC7466
SP261 (TIGR4)	4	None	[8]
SP309 (G54)	19F	None	[9]
SP313 (R6)	NC ^c	None	[10]
SP332	1	None	[11]
PN111	D39Δ <i>cps</i>	Km ^r	[12]
PN149	D39 <i>lux</i>	Km ^r	[13]
PN220	D39Δ <i>cps</i> Δ <i>lgt</i>	Km ^r , Erm ^r	[14]
PN319	D39Δ <i>cps</i> Δ <i>cbpL</i>	Km ^r , Erm ^r	This work
PN329	D39 <i>lux</i> Δ <i>cbpL</i>	Km ^r , Erm ^r	This work
PN259	TIGR4Δ <i>cps</i>	Km ^r , Erm ^r	[15]
PN443	TIGR4Δ <i>cps</i> Δ <i>lgt</i>	Km ^r , Erm ^r	This work
PN249	TIGR4Δ <i>cps</i> Δ <i>cbpL</i>	Km ^r , Erm ^r	This work
<i>Escherichia coli</i>			
DH5α	Δ(<i>lac</i>)U169, <i>endA1</i> , <i>gyrA46</i> , <i>hsdR17</i> , Φ80Δ(<i>lacZ</i>)M15, <i>recA1</i> , <i>relA1</i> , <i>supE44</i> , <i>thi-1</i>	None	Novagen
BL21 (DE3)	<i>E. coli</i> B, F- <i>dcm ompT hsdS gal λ</i> (DE3), T7 polymerase gene under control of the <i>lacUV5</i> promoter	None	Stratagene
Plasmids			
pGEM-T Easy	TA cloning vector for PCR products; Ap ^r	Ap ^r	Promega
pE89	pCR2.1Topo derivative with erythromycin cassette	Ap ^r , Km ^r , Erm ^r	[16]
p562	pGEM-T derivative with <i>sp_0667</i> + 5' and 3' flanking region for mutagenesis (TIGR4-derived strains)	Ap ^r	This work
p569	pGEM-T derivative with <i>sp_0667</i> interrupted by Erm resistance cassette (TIGR4-derived strains)	Ap ^r , Erm ^r	This work
p716	pGEM-T derivative with <i>spd_0579</i> + 5' and 3' flanking region for mutagenesis (D39-derived strains)	Ap ^r	This work
p717	pGEM-T derivative with <i>spd_0579</i> interrupted by Erm resistance cassette (D39-derived strains)	Ap ^r , Erm ^r	This work
pET28a	Protein expression vector	Km ^r	Novagen
pTP1	pET28a derivative expression vector	Km ^r , Erm ^r	[6]
p630	pET28TEV derivative with TIGR4 <i>sp_0667</i> (<i>cbpL</i>) for protein production and mice immunization	Km ^r	This work
p718	pET28TEV derivative with TIGR4 <i>sp_0667</i> (<i>cbpL</i>) for protein production	Km ^r	This work
p1025	pET28TEV derivative with TIGR4 <i>sp_0667</i> w/o Ltp for protein production	Km ^r	This work
p1070	pET28TEV derivative with TIGR4 Excalibur_ <i>sp_0667</i> for protein production	Km ^r	This work

^aAp, ampicillin; Km, kanamycin; Erm, erythromycin; r, resistant

^bMUD, Medical University of Düsseldorf, Germany

^cNC, nonencapsulated strain

Table S2. Primer list

Primer intended use	Primer name	Sequence (5'-3')
Insertion-deletion mutagenesis		
Amplification of <i>sp_0667</i> + 5' and 3' flanking region (D39-derived strains)	CbpL_632	5'-ACTAGAATTCGACAAAAGATAGAGGCGGA-3'
	CbpL_409	5'-AACCTTCCAAGCTGCAGCTGCTGCACCAGCAACA-3'
Amplification of <i>sp_0667</i> + 5' and 3' flanking region (TIGR4-derived strains)	CbpL_406	5'-CTACTACTAGAATTCTGCATGGGTTAGGGCAGT-3'
	CbpL_409	5'-AACCTTCCAAGCTGCAGCTGCTGCACCAGCAACA-3'
Inverse PCR of <i>sp_0667</i> + 5' and 3' flanking region (pGEMTeasy)	CbpL_408	5'-ACTCACTCACTGCTCGAGTGCAGTCAATATGCCATT-3'
	CbpL_407	5'-ATCATCATCATCGGGTACCCTTTATTTCATTTCTTCTCCATA-3'
Antibiotic cassette amplification		
erythromycin (<i>ermB</i>)	ermB_105	5'-GATGATGATGATCCCGGTACCAAGCTTGAATTCACG GTTCTGTTCGTGCTG-3'
	ermB_106	5'-AGTGAGTGAGTCCCGGGCTCGAGAAGCTTGA ATTCTAGGCGCTAGGGACCTC-3'
Recombinant protein production and vector modification		
<i>sp_0667</i> (TIGR4) His-tag-protein	CbpL_461	5'-GCGCGCTAGCGAAGAAAACATCCATTTTTTC-3'
	CbpL_462	5'-GGCCGAGCTCTTAATCATCTAAATGATCAATGG-3'
<i>sp_0667</i> (TIGR4) untagged protein	CbpL_598	5'-GCGCCCATGGGAAGAAAACATCCATTTTTTC-3'
	CbpL_462	5'-GGCCGAGCTCTTAATCATCTAAATGATCAATGG-3'
<i>sp_0667</i> (TIGR4) Excalibur domain	CbpL_461	5'-GCGCCCATGGGAAGAAAACATCCATTTTTTC-3'
	CbpL_1156	5'-GGCCGAGCTCTAATTTTTCAATTCGCAAGCCAC-3'
<i>sp_0667</i> (TIGR4) Excalibur-CBM (w/o Ltp) His-tag-protein	CbpL_461	5'-GCGCCCATGGGAAGAAAACATCCATTTTTTC-3'
	CbpL_1321	5'-GCGCGAGCTCGCTATCATTACTAGAAAGAGCT-3'
<i>sp_0667</i> (TIGR4)	CbpL_1470	5'-GCGCGCGCTAGCGCTCCTAAGGGTGCTTTTAA-3'

^a Restriction sites are underlined